



Minerva Access is the Institutional Repository of The University of Melbourne

Author/s:

Kearney, MR

Title:

How will snow alter exposure of organisms to cold stress under climate warming?

Date:

2020-07-01

Citation:

Kearney, M. R. (2020). How will snow alter exposure of organisms to cold stress under climate warming?. *GLOBAL ECOLOGY AND BIOGEOGRAPHY*, 29 (7), pp.1246-1256. <https://doi.org/10.1111/geb.13100>.

Persistent Link:

<https://hdl.handle.net/11343/275617>

Title: How will snow alter exposure of organisms to cold stress under climate warming?

Running head: Snow, climate warming and cold stress

Michael R. Kearney

School of BioSciences, The University of Melbourne, Victoria 3010, Australia

Corresponding author: Michael Kearney, School of BioSciences, The University of Melbourne, Victoria 3010, Australia. Phone (613) 8344 4864, email m.kearney@unimelb.edu.au

Acknowledgements

I thank Warren Porter, Ray Huey, Megan Fitzpatrick and Kat Borman for discussion and suggestions.

Biosketch

Michael Kearney is an ecophysiologicalist whose research focuses on integrating physical and biological principles to understand constraints on the behaviour, distribution and abundance of organisms. He is developing the NicheMapR package, a suite of programs in the R environment for modelling microclimates and their consequences for the heat, water and dynamic energy budgets of organisms.

Data availability

All data used in this study are publicly available and all required code to generate the results are publicly available and open source.

This is the author manuscript accepted for publication and has undergone full peer review but has not been through the copyediting, typesetting, pagination and proofreading process, which may lead to differences between this version and the [Version of Record](#). Please cite this article as [doi: 10.1111/GEB.13100](https://doi.org/10.1111/GEB.13100)

This article is protected by copyright. All rights reserved

1
2
3
4
5
6
7
8
9
10
11
12
13
14
15
16
17
18
19
20
21
22
23
24
25
26
27
28
29
30

DR. MICHAEL R. KEARNEY (Orcid ID : 0000-0002-3349-8744)

Article type : Research Papers

Title: How will snow alter exposure of organisms to cold stress under climate warming?

Running head: Snow, climate warming and cold stress

Abstract

Aim: To test the capacity of an ecologically-focussed microclimate model to capture the interaction between snow cover and soil temperature and use it to assess how historical and future climate warming affects exposure of organisms to stressfully cold conditions in shallow soil.

Location: continental USA

Time Period: 1980 to 2017

Method: A snow heat budget algorithm was developed and integrated with the general-purpose microclimate model of the NicheMapR package. The gridMET daily historical weather grids were used as environmental forcing. The model was tested against hourly observations of soil temperature and snow cover for 590 SCAN/SNOTEL sites across the USA. It was then used to simulate ectotherm cold stress exposure and endotherm hibernation costs.

Results: The model captured soil and snow observations to within ~10-15 % of the range ($r \sim 0.85$). Air temperature exhibited a mean warming rate of 0.37 °C per decade across sites but in snow affected regions the predicted shallow-soil warming rates were one third lower. Biophysical analyses predicted increased activity ectotherm time as a result of contemporary climate change but little change in cold stress at most sites. For endotherms, hibernation costs were predicted to decline in

31 general. However, both reduced and increased cold stress was simulated to occur for ectotherm and
32 endotherms under simulated air temperature warming of up to 3 °C.

33

34 Main conclusions: Many of the direct biological consequences of climate warming will be mediated
35 through soil temperature. Microclimatic processes linked to snow cover mean that exposure to cold
36 stress for both ectotherms and endotherms may stay constant, decrease or even increase under
37 climate warming depending on the local circumstances and species-specific biology. The
38 idiosyncratic and season-specific decoupling of above- and below-ground environments under
39 climate warming will have important ecological consequences in snow-affected regions and can now
40 be computed mechanistically.

41

42 **Key Words:** snow, soil temperature, cold stress, hibernation, microclimate, NicheMapR, SCAN,
43 SNOTEL, climate warming

44

45 **Introduction**

46 Snow has long been known for its ecological importance. Snow protects plants from exposure to
47 cold and from desiccating winds, as well as contracting the growing season (Warming, 1909). Many
48 cold-adapted animal and plant species rely on the stable, moist subnivean conditions that occur near
49 the ground-snow interface during winter (Pauli *et al.*, 2013). Snow-mediated soil temperatures can
50 also affect microbial dynamics with consequences for carbon cycling (Monson *et al.*, 2006). Climate
51 warming will increase growing season length in cold environments but any associated reductions in
52 snow depth and duration may increase exposure to extremely cold microclimates and outweigh any
53 positive effects (Wipf *et al.*, 2009). For example, climate warming may increase activity time for
54 ectotherms (Kearney, 2013) but reduced snow cover may increase exposure to extreme cold (Bale &
55 Hayward, 2010). During the snow season, many endotherms enter hibernation where body
56 temperature and hence energy requirements are dramatically reduced (e.g. Körtner & Geiser, 1998).
57 Climate warming may reduce the overall hibernation period by reducing snow cover, but shallower
58 snow may mean that hibernating endotherms experience colder conditions, with complex
59 consequences for their energy budgets. Thus whole communities dependent on the ‘subnivium’ will
60 be strongly affected by snow-mediated microclimatic effects of climate change (Ávila-Jiménez *et al.*,
61 2010; Pauli *et al.*, 2013; Sanders-DeMott *et al.*, 2018, 2019) and we therefore need good models of
62 how snow affects soil temperatures if we are to predict the ecological consequences.

63

64 The interaction between climate change, snow, soil temperature and other microclimatic conditions
65 is highly multidimensional and non-linear (Zhang, 2005; Zhang *et al.*, 2005; Thompson *et al.*, 2018).
66 The ultimate outcome of climate warming in snow-affected areas will depend on the balance
67 between the buffering effect of snow and the overall addition of heat to the soil profile (Campbell *et al.*,
68 2010; Aalto *et al.*, 2018). In certain circumstances, snow melt as a result of a warming climate
69 may result in paradoxical cooling of soil with the warming of air (Groffman *et al.*, 2001; Decker *et al.*,
70 2003; Isard *et al.*, 2007; Sinha & Cherkauer, 2010; Brown & DeGaetano, 2011).

71 How can we incorporate these complexities introduced by snow cover into our understanding of
72 species responses to climate change? One approach is to empirically compare spatially broad time
73 series of snow cover and soil temperature data to better understand their interaction. In the USA,
74 the Soil Climate Network Analysis (SCAN, Schaefer *et al.*, 2007) and SNOw TElemetry (SNOTEL,
75 Serreze *et al.*, 1999) projects comprise over 600 stations recording snow and soil conditions dating
76 back to the 1960s. However, it is difficult to infer the general nature of climate-snow-microclimate
77 interactions from these sources because of data incompleteness, especially for concurrent
78 measurements of soil temperature, snow cover and air temperature. Thus, in this study I take a
79 simulation approach by forcing a general microclimate model with historical gridded data, using the
80 historical point-observations to test model performance. I then use the simulation results to assess
81 the consequences of historical climate change and future potential warming for the snow/soil
82 temperature interaction, and their ecological consequences for ectotherms and endotherms.

83
84 Several modelling approaches have been developed for predicting soil temperature as a function of
85 snow cover (e.g. Jordan, 1991; Liston & Sturm, 1998; Zhang, 2003; Anderson, 2006; Bartlett *et al.*,
86 2006; Essery *et al.*, 2013; Avanzi *et al.*, 2016; Lute & Luce, 2017; Cuntz & Haverd, 2018; Hamman *et al.*,
87 2018). These approaches range from fully physical schemes that explicitly consider energy and
88 mass balances, to more phenomenological approaches that use descriptive formulations. Most
89 ecologically-focused studies of microclimatic snow effects have been in the middle of this spectrum,
90 balancing data input requirements with model transferability. For example, Isard *et al.* (2007) and
91 Brown *et al.* (2011) integrated soil heat flow models with snow and soil moisture models in such a
92 way that only air temperature and rainfall data were needed as forcing data. However, radiation and
93 humidity interact in complex ways to affect snow cover (Harpold & Brooks, 2018) and more
94 mechanistic approaches are therefore desirable.

95
96 In this study I use a fully physical microclimate model that simultaneously solves a complete energy
97 and mass budget for the soil and snow profile, and uses radiation, wind and humidity forcing data in

98 addition to air temperature and precipitation (NicheMapR, Kearney & Porter, 2017). This modelling
99 framework is more generalisable than phenomenological ones, and more targeted to ecological-
100 scale outputs (hourly time-step, fine-scale topographic adjustments, detailed soil profiles) than are
101 Land Surface Models. Moreover, the NicheMapR package also includes algorithms for computing the
102 biophysical consequences of microclimates for different kinds of organisms (Kearney & Porter,
103 2019).

104
105 Microclimate models can now be applied on broad spatial scales at fine temporal resolution due to
106 the increasing availability of historical gridded meteorological forcing data (New *et al.*, 2002; Jones *et al.*,
107 2009; Kemp *et al.*, 2012; Abatzoglou, 2013). I integrated the NicheMapR microclimate with the
108 gridMET historical climatology of the USA (Abatzoglou, 2013) and the data from 590 SCAN/SNOTEL
109 sites (Schaefer *et al.*, 2007) to test the model's performance and to quantify the buffering influence
110 of snow on soil temperature across continental USA as well as the pattern of historical change in
111 shallow (5cm) soil temperature in relation to air temperature and snow cover. I then used the model
112 output to explore the potential effects of snow on shallow soil temperature and the physiological
113 consequences of these effects for ectotherms and endotherms. Specifically, I address the following
114 questions: 1) To what extent are soil temperatures independent of, or reduced by, climate warming
115 through the buffering effect of snow? 2) How will climate warming affect exposure to cold stress in
116 overwintering ectotherms? and 3) How will climate warming affect the energetic costs of
117 hibernation in endotherms?

118 119 **Materials and Methods**

120 **Snow model formulation**

121 All simulations were done with the microclimate model of the NicheMapR package, now fully open
122 source (<https://github.com/mrke/NicheMapR>). The model can be installed and run for the USA from
123 base R in 5 lines of code, with all meteorological forcing data accessible online via opendap (SI
124 Supplementary Text). The snow model of the NicheMapR microclimate model was partially
125 described by Kearney and Porter (2017) and here I provide an overview and additional details. Snow
126 layers form an extension of a maximum of eight nodes above the ten nodes used to compute heat
127 flux through the soil profile. These additional snow nodes are at 2.5, 5, 10, 20, 50, 100, 200 and
128 300cm, with the original soil surface node (0cm) acting as the snow surface node and the connection
129 between the 300cm snow node and the depth of the soil surface node being allowed to grow to an
130 arbitrary large extent. As the snow pack grows and shrinks, the subroutine 'snowlayer' checks
131 whether to increase or decrease the number of snow nodes in use. Snow is set to zero if the

132 predicted depth is less than 2.5 cm to ensure numerical stability but small rainfall events that would
133 otherwise produce a snow layer shallower than this threshold are cumulated each hour until the
134 threshold is met, conserving mass balance. Snow growth is driven by inputted precipitation for each
135 day (or hour, if hourly rainfall data are available) and by the user-specified thresholds for the air
136 temperature at which rain falls as snow. Snow density ρ_{snow} can be constant, vary as a linear
137 function of snow age (with a maximum of 0.9167 Mg/m³), or can vary with the non-linear asymptotic
138 formulation of Sturm *et al.* (2010, eq. 5) $\rho_{snow} = (\rho_{max} - \rho_0)[1 - \exp(-k_1h - k_2D)] + \rho_0$ where
139 ρ_{max} is the maximum allowable density, ρ_0 is the initial density, k_1 and k_2 are fitting parameters, h
140 is the snow height (cm) and D is the age of the snow (days; note that this differs from Sturm *et al.*
141 (2010) in that they used D as day of year). The latter function was used in all analyses presented
142 here, using the parameters $\rho_{max} = 0.9167$, $\rho_0 = 0.27$, $k_1 = 0.004$ and $k_2 = 0.009$.

143
144 All snow for a given day is assumed to fall at midnight if the rainfall input is daily (as in the present
145 case), and the user can specify a multiplier to account for undercatch (wind-driven precipitation
146 inaccuracies) if necessary (Rasmussen et al. 2012). When snow is present, the fractional surface
147 albedo α changes as a function of the age of the snow pack as $\alpha = -9.8740 \ln(d_{snow} + 78.3434)$
148 where d_{snow} is the days since the last snowfall based on regressions fitted to Fig A-4 of Anderson
149 (2006), and reverts to the user-specified value for the substrate when snow is absent. Snow thermal
150 conductivity is estimated from Djachkova's formula following Anderson (2006) $k_{snow} =$
151 $0.0442e^{5.181\rho_{snow}}$. Snow melt occurs according to the heat load as computed by the heat budget for
152 the substrate (including the snow), as well as melting due to rain. If there is a temperature increase
153 between time steps for a given internode of the snowpack, this temperature difference is multiplied
154 by the snow heat capacity (including the heat of fusion), snow density and distance between the
155 nodes to obtain the heat input, and then divided by the heat of fusion to compute the mass of snow
156 melted, with temperatures of the respective nodes set to 0 °C. Rain-melt is simulated following
157 Anderson (2006) by multiplying the product of the rainfall and mean air temperature for the day by
158 a rain melt factor (default value 0.0125) whenever rain falls at air temperatures above the snow
159 threshold (this is the only phenomenological aspect of the model).

160

161 **Environmental Forcing data**

162 Meteorological forcing data were obtained from the gridMET dataset of 0.042° (~4 km) resolution
163 daily grids of minimum and maximum air temperature, minimum and maximum relative humidity,
164 daily cumulative precipitation, daily cumulative solar radiation and mean daily wind speed. Observed
165 solar radiation was converted into a fraction of the maximum possible for each day under clear sky

166 conditions using the `micro_global` function of the NicheMapR package, and used as cloud cover as
167 per Kearney et al. (2014). Air temperature was adjusted via lapse rate corrections of $0.0039\text{ }^{\circ}\text{C m}^{-1}$
168 and $0.0077\text{ }^{\circ}\text{C m}^{-1}$ for minimum and maximum temperature, respectively (Ruddell *et al.*, 1990), for
169 the reported elevation at each site, with relative humidity then recomputed for the new
170 temperature. Soil properties were extracted from the SoilGrids global dataset (Hengl *et al.*, 2014,
171 2017), a $\sim 250\text{m}$ resolution product, using the `jsonlite` package. Soil bulk density, and percent sand,
172 silt and clay were extracted for 0, 5, 15, 30, 60, 100 and 200 cm and converted to soil hydraulic
173 parameters (air entry potential, saturated hydraulic conductivity and Campbell's b) using the
174 'pedotransfer' function of the NicheMapR package that is based on Cosby et al. (1984), as described
175 in more detail in Kearney and Maino (2018). These connections to the gridMET and SoilGrids data
176 are encoded in a new function in the NicheMapR package, 'micro_usa'.

177

178 **Sites and observation data**

179 The model was tested at 590 SCAN and SNOTEL sites with time-series of snow depth, snow water
180 equivalent (SWE), soil temperature and soil moisture (5, 10, 20, 50 and 100 cm) observations for
181 between 0.9 and 24.4 years (mean 13.8). Two test scenarios were run. In the first scenario, slope,
182 aspect, shading and horizon angles were all assumed to be zero. In the second scenario, these
183 parameters were adjusted based on assessments of site photos available at
184 <https://www.wcc.nrcs.usda.gov/scan/>. Each photo was used to estimate canopy shade level (to
185 nearest 5%), slope (to nearest 5%), horizon angles (to nearest 5%, assumed either uniform in all 24
186 directions, or alternative between a single estimated value and zero in sites deemed as woodland),
187 whether the substrate was rock or soil (used to determine whether an organic cap was absent or
188 present, respectively), and the proportion of ground cover (nearest 5%) (Table S1). The ground cover
189 fraction was used as an estimate of shade, but this shade was only imposed if no snow was present,
190 on the assumption that the groundcover was under the snow. In addition, a preliminary run of the
191 model for the year 2017 (using 2016 as a spin-up year) for all sites was done across all 11 soil types
192 in Table 9.1 of Campbell and Norman (Campbell & Norman, 1998), and the best fitting hydraulic
193 parameter set was used for each respective soil layer for the final simulation. All other parameters
194 for the microclimate model were set to the default values to be found in the 'micro_usa' function.

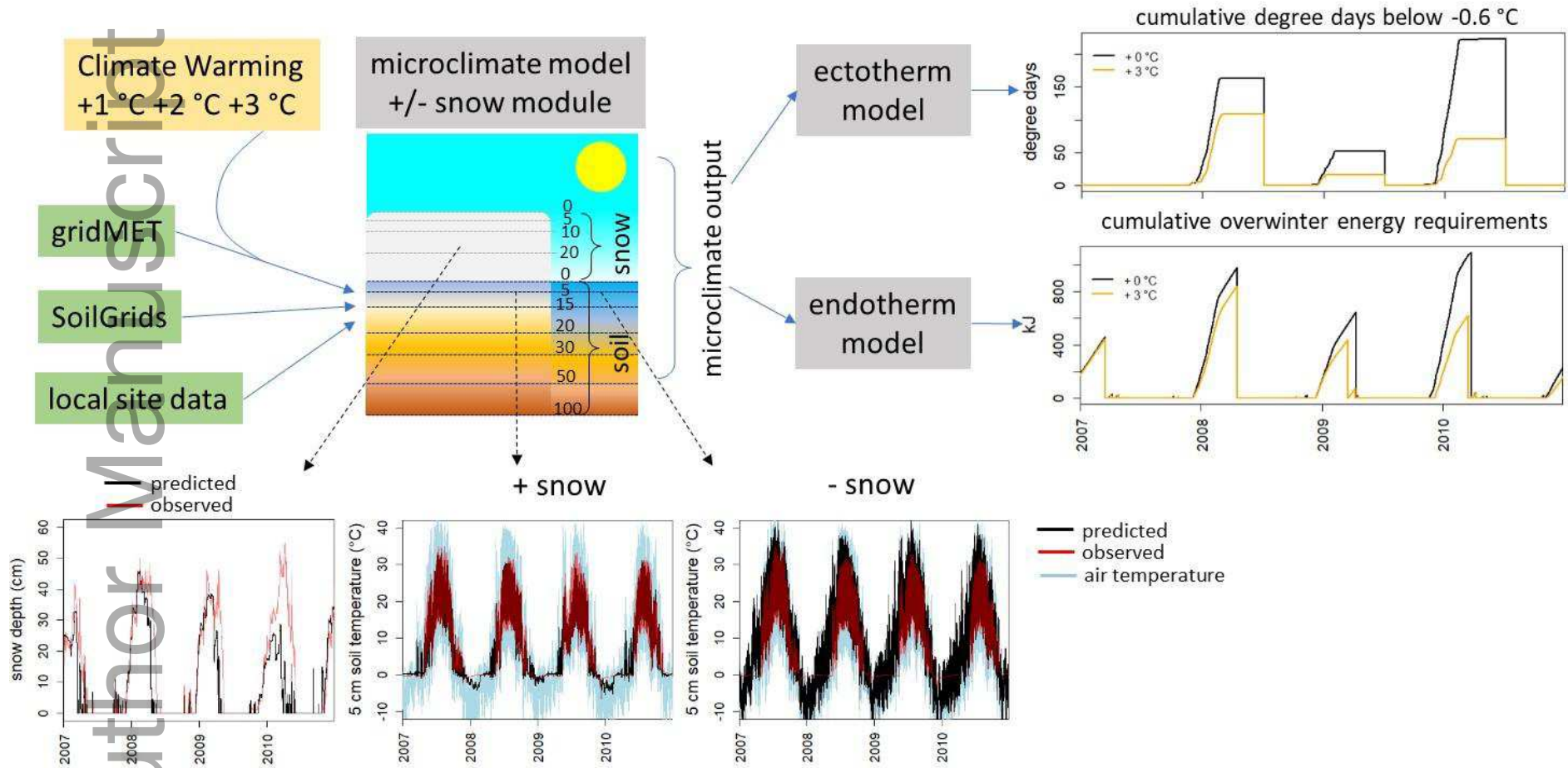
195

196 **Simulations and Analyses**

197 A schematic of the overall simulation approach is shown in Figure 1. The model was run at all sites
198 for the years 1979 to 2017 (the year 1979 used as a 'spin-up' year), with the soil depth nodes chosen
199 to match the observation data (5, 10, 20, 50 and 100 cm - the depths were measured in inches and

200 approximate the cm depths here). A total of six different scenarios were considered. First
201 (DefaultTest) the model was run with all default settings and using the SoilGrids database for soil
202 hydraulic properties. Second (LocalTest), it was run as in DefaultTest but with parameters adjusted
203 as described in the section above, to match the local conditions as indicated in site photos and to
204 use the best-fitting soil type for hydraulic properties. Third, the model was run with the snow
205 module switched off (NoSnow), so that instead of precipitation falling as snow it fell as rain and only
206 affected soil temperature via its effect on soil moisture. Finally, simulations were run incrementing
207 the air temperature by one degree to a maximum of three degrees higher than base level (Warm1,
208 Warm2 and Warm3). The latter four simulations used the DefaultTest settings to obtain a picture of
209 the effect of snow and warming with all else being equal.

Author Manuscript



211

212 Figure 1. Overview of the scheme for modelling snow-mediated microclimatic effects on organisms using the NicheMapR package. The environmental data
 213 (green boxes) includes forcing weather data (gridMET for the USA), soil characteristics (sourced from the SoilGrids database) and local site information on
 214 topography, shading etc. The microclimate model predicts above- and below-ground environments, including the accumulation and melting of snow and its

215 influence on ground temperature. The snow model can be turned on or off to study the direct effect of snow. The outputs of the microclimate model can
216 then be used to simulate the biophysical consequences for ectotherms (e.g. cumulative exposure to below-zero body temperature for a given winter) and
217 endotherms (e.g. hibernation energy costs of overwintering). Example simulations (back, blue) and observations (red) are given for Dorsey Basin, Nevada
218 USA (SNOTEL site 453) and the consequences for ectotherms and endotherms are shown for current climate (black) and a uniform warming of 3 °C
219 (orange). The code to generate these simulations is provided in the Supplementary Text.

220

221 For each simulation, hourly output of reference (2 m) and local (1 cm above surface, i.e. of soil or of
222 snow if present) air temperatures were saved as well as estimates of snow depth, snow density, and
223 soil temperature and moisture at each depth. The hourly model predictions for DefaultTest and
224 LocalTest were compared to hourly observations using the correlation coefficient r and the root
225 mean square deviation $rmsd$, as in Kearney and Maino (2018), as well as the $rmsdp$ ($rmsd/range$,
226 expressed as %) and mean bias error. Observation data were filtered to remove negative values (for
227 snow depth, snow water equivalent and soil moisture), and hourly spikes above or below a threshold
228 level (> 20 cm for snow depth, > 20 inch for snow water equivalent, > 5% for soil moisture and > 20
229 °C for temperature) (see also Avanzi *et al.*, 2014). All observation data sets were checked for
230 aberrant data and variables were excluded from analyses where necessary; these were sites with
231 clearly impossible values (some likely due to incorrect units, e.g. °F rather than °C, and others
232 apparently due to sensor mix-up, e.g. highly fluctuating temperatures in deep soil).
233 The hourly air temperature (1 cm and 2 m), snow depth and soil temperature data from DefaultTest,
234 NoSnow and Warm1-3 were then aggregated to provide annual summary statistics of snow depth,
235 snow days, air and soil temperature and degree days below 0 °C per height/depth, offsetting by half
236 a year to ensure that statistics referred to a whole winter. Where annual means are presented, these
237 are the means of the aggregated yearly values. Linear regression analysis of relationships between
238 these variables with year and with each other were undertaken and the slopes, R^2 and P -values
239 saved (all mapped results are for cases where $P < 0.05$).

240

241 Finally, two example biophysical simulations were run to assess the physiological consequences of
242 snow-mediated soil temperatures under the DefaultTest and Warm1-3 scenarios. First, a simulation
243 of a 20 g thermoregulating lizard was run using the 'ectotherm' model of the NicheMapR package
244 (Kearney & Porter, 2019). The activity body temperature range was assumed to be 32-37 °C,
245 between 0 and 90% shade could be selected when active and the retreat site was at 5 cm below the
246 soil surface. Annual activity time and exposure to cold stress (degree days below super-cooled body
247 temperature of -0.63 °C) was then collated. Second, the total energy requirements of a hibernating
248 20 g endotherm at 5 cm depth was simulated during periods of snow cover using the 'ellipsoid'
249 function of NicheMapR (Porter & Kearney, 2009). The required metabolic rate to balance the heat
250 budget at basal metabolic rate (BMR) for core temperatures ranging from 2 to 20 °C in 1 °C
251 increments was computed for all hours that snow cover was > 5 cm depth (assuming this
252 represented times when food was inaccessible). Basal metabolic rate was adjusted from the
253 expected normothermic value at 37 °C to the simulated body temperature using a typical Q10 of 2.5

254 (Geiser, 2004). For each hour, the core temperature that resulted in the lowest BMR was chosen and
255 the overall trajectory then summed for a given winter to obtain the total energetic cost of
256 hibernation (See Supplementary Text for all ectotherm and endotherm model parameters).

257

258 **Results**

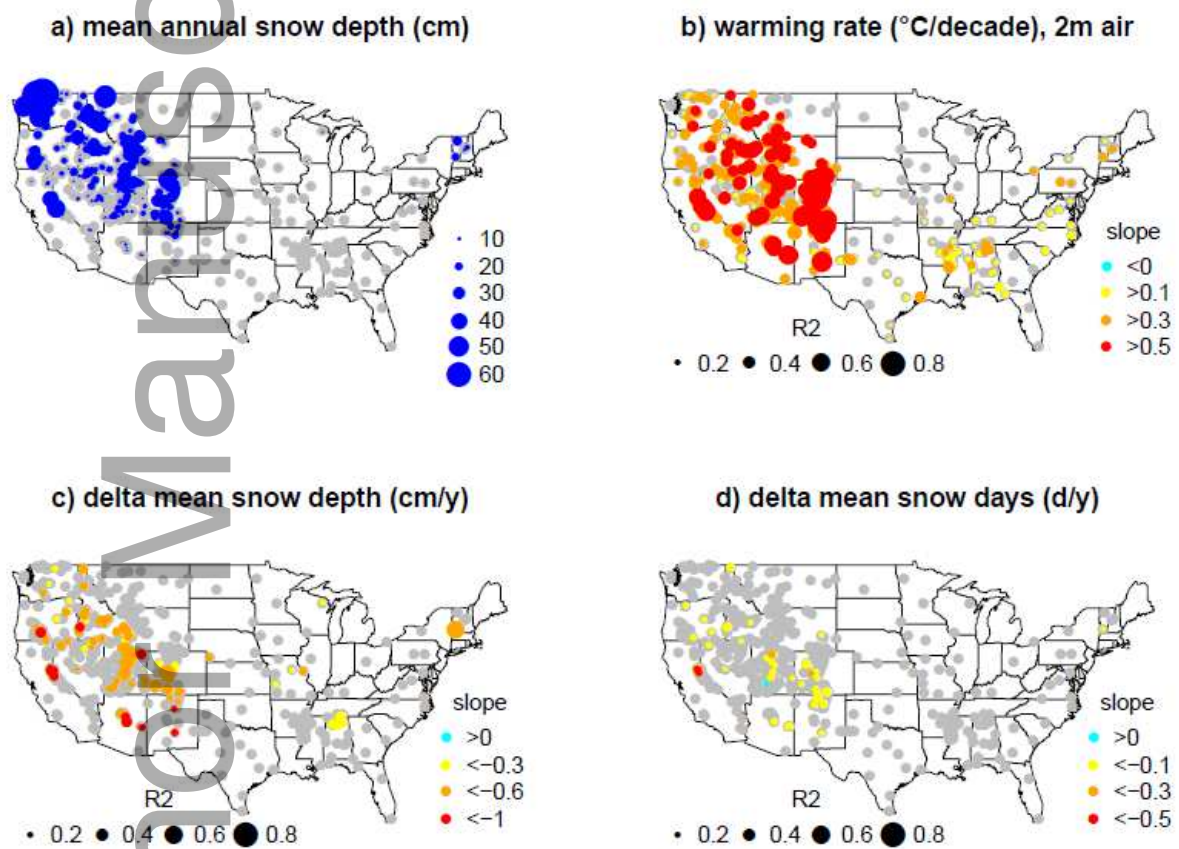
259 Tests of the model predictions of snow depth and SWE were within 15% of the observed range and
260 highly correlated with the observations ($r \sim 0.85$), with the model skill and bias (slightly positive)
261 differing little between DefaultTest (default settings) and LocalTest (shade, soil and terrain tuned to
262 local site conditions) (Table 1). Soil temperature predictions showed similar skill, being within
263 between 10% and 15% of observed ranges across all depths to 50 cm and showing high correlation
264 with the observations (r 0.83-0.96) and a small positive bias. Predictions of 100 cm soil temperature
265 had lower skill, especially for LocalTest (Table 1). Again, little difference was found in model
266 performance between DefaultTest and LocalTest. Soil moisture predictions were within $\sim 27\%$ of
267 observed ranges for depths down to 50 cm under DefaultTest but this improved to $\sim 20\%$ under
268 LocalTest ($r \sim 0.6$ in both tests) and bias was substantially reduced, again with 100 cm predictions
269 being of lower skill (Table 1). Figure 1 shows a typical match between time series of observed and
270 predicted snow depth and snow temperature. Simulated snow removal reduced minimum soil
271 temperature by around 10°C , and in some places by as much as 19°C (Fig. 1 & Fig. S1). Histograms
272 of the summary statistics per site for DefaultTest and LocalTest are provided in Appendix S1, and
273 plots of observed and predicted values for all 590 sites for snow, soil temperature and soil moisture
274 (DefaultTest) are in Appendices S2, S3 and S4, respectively.

275

276 **Table 1.** Correlation coefficients (r), root mean square deviation ($rmsd$), percent root mean square deviation ($rmsdp$) and bias error ($bias$) for hourly snow
 277 depth (cm), snow water equivalent (SWE), soil temperature (T_{soil}) and soil moisture (M_{soil}) at different depths under DefaultTest (default settings) and
 278 LocalTest (shade, soil and terrain matched to local conditions).

	DefaultTest				LocalTest			
	r	$rmsd$	$rmsdp$	$bias$	r	$rmsd$	$rmsdp$	$bias$
snow depth (cm)	0.86	9.15	14.32	1.34	0.86	9.43	14.7	1.13
T_{soil} 5 cm (°C)	0.87	4.81	12.66	0.21	0.88	4.45	11.81	0.24
T_{soil} 10 cm (°C)	0.94	3.60	10.02	0.81	0.95	3.49	9.65	1.02
				-				
T_{soil} 20 cm (°C)	0.96	2.62	9.92	0.11	0.96	2.54	9.91	0.00
T_{soil} 50 cm (°C)	0.92	2.57	13.47	0.07	0.89	2.81	15.18	0.27
T_{soil} 100 cm (°C)	0.67	4.26	21.91	1.27	0.58	4.57	24.4	1.35
				-				-
M_{soil} 5 cm (%vol)	0.59	10.69	27.89	6.55	0.59	7.99	19.96	0.27
				-				
M_{soil} 10 cm (%vol)	0.61	8.71	24.58	2.12	0.62	6.95	18.87	0.35
				-				-
M_{soil} 20 cm (%vol)	0.61	9.39	26.41	2.20	0.61	7.2	20.68	0.06
				-				
M_{soil} 50 cm (%vol)	0.56	9.92	29.32	0.52	0.58	7.05	23.00	0.49
M_{soil} 100 cm (%vol)	0.46	11.16	37.31	2.74	0.45	9.47	32.91	2.94

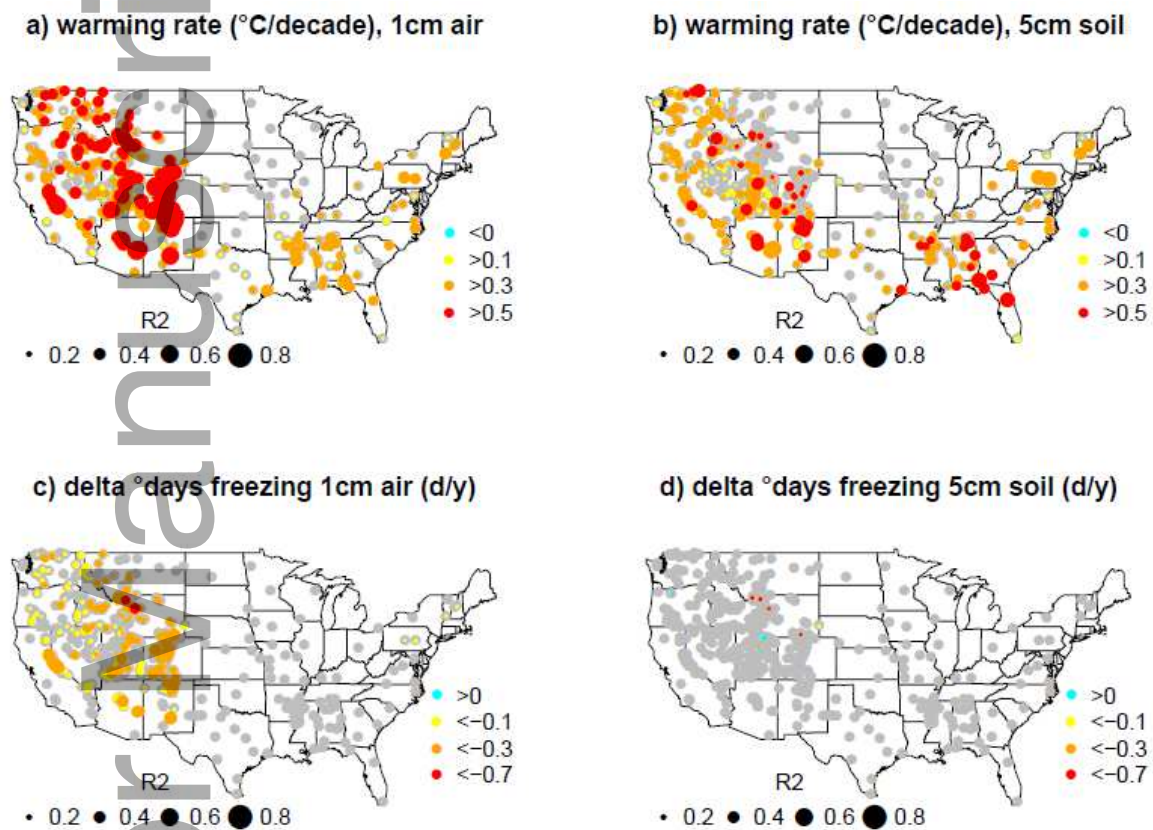
279 Of the 590 SCAN/SNOTEL sites, 286 were simulated to have a mean annual snow depth of > 10 cm
 280 and these were clustered in the northwest (Fig. 2a) consistent with the empirical observations (Fig.
 281 S2a). The rate of warming of 2 m gridMET air temperatures exceeded 0.1 °C per decade at 87.1 % of
 282 sites and 0.5 °C per decade at 21.3 % of sites; over 75% of the latter sites were simulated to have >
 283 10 cm mean annual snow depth per year (Fig. 2b, see Fig. S2b for local station observations and also
 284 Harpold & Brooks, 2018). Of the snow sites, 32 % showed linear declines in snow depth over the
 285 simulation period ($R^2 > 0.1$, slope < -0.3 cm/y) (Fig. 2c) and 12% showed linear declines in duration
 286 (Fig. 2d).
 287



288
 289 **Figure 2.** Simulation outputs (DefaultTest) of a) mean annual snow depth, b) annual warming rate of
 290 2m air temperature, c) rate of change in mean annual snow depth and d) rate of change in mean
 291 annual snow duration across the USA between 1980 and 2017. Grey points indicate sites with
 292 magnitude zero. Figure S2 shows the equivalent figures for raw observational data.

293
 294 The simulated 1 cm air temperature showed a similar pattern to the 2 m air temperature change
 295 with 21.5 % of sites exhibiting warming rates of > 0.5 °C (with an $R^2 > 0.1$ for the linear regression of
 296 warming on year, Fig. 3a). But in the soil at 5 cm depth, only 9.1 % sites showed warming rates > 0.5
 297 °C (Fig. 3b). Similarly, the reduction in degree days of subzero 1 cm air temperatures was more than

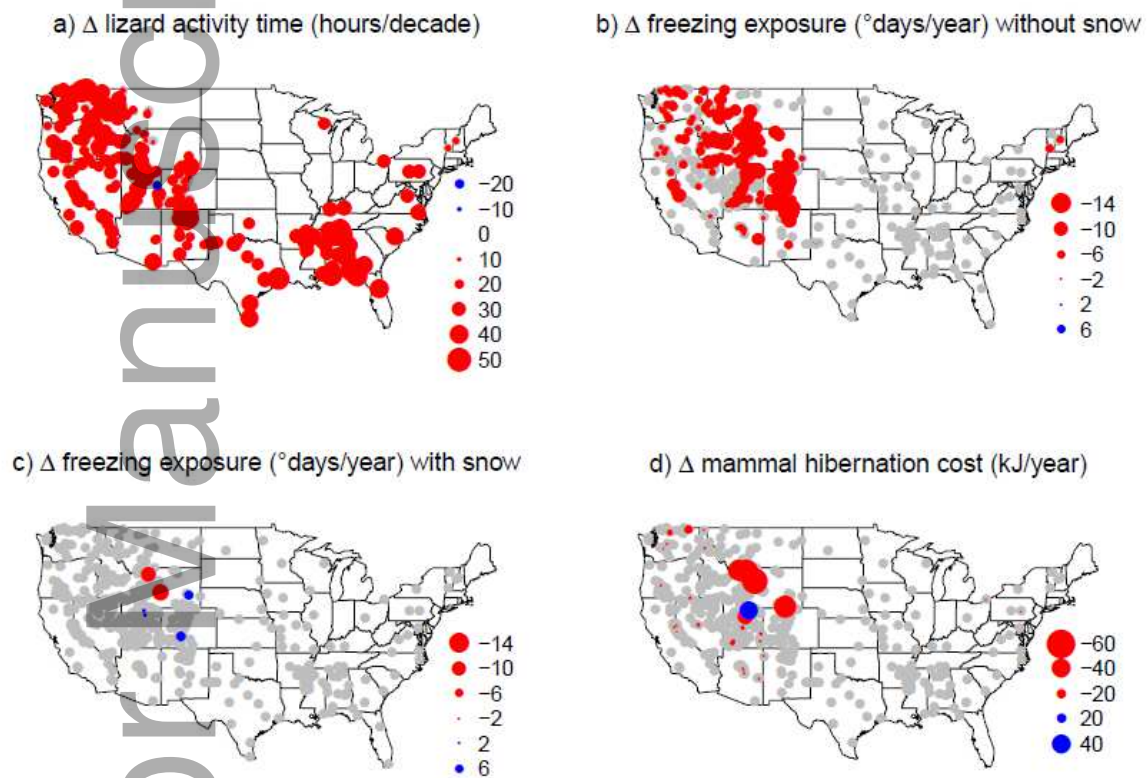
298 0.3 days per year at 50.7% of sites but for 5 cm soil this only occurred for 1.5 % of sites (Fig. 3c & d).
 299 Comparison of these patterns with those when the snow model was turned off show that the
 300 divergent responses of soil and air temperatures is attributable to the buffering effect of snow; i.e. in
 301 the absence of snow for 5 cm soil, the proportion of sites with warming rates > 0.5 °C increased to
 302 38.3 % and the number of sites with reductions in degree days of subzero exposure increased to
 303 65.4 % (Fig. S3).
 304



305
 306 **Figure 3.** Simulated change in decadal warming rate of a) 1 cm air temperature and b) 5 cm soil
 307 temperature as well as change in degree days below 0 °C of c) 1 cm air temperature and d) 5 cm soil
 308 temperature across the USA between 1980 and 2017. Grey points indicate sites with magnitude
 309 zero. Figure S3 shows the equivalent figures with the snow model turned off.

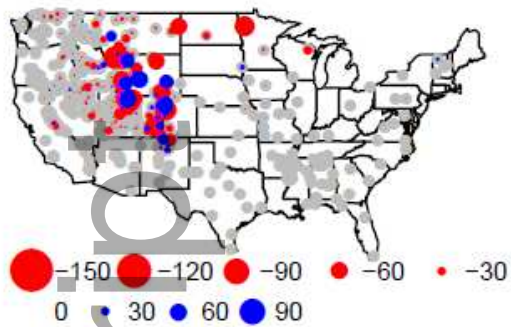
310
 311 Biophysical simulations of a thermoregulating lizard experiencing conditions 1 cm above ground
 312 show that historical warming has increased potential activity time across 57.4 % of sites, in some
 313 cases by over 50 hours per decade (Fig. 4a), consistent with historical air temperature increases
 314 (Figs. 2b & S2b). When the snow model was turned off, contemporary climate warming caused
 315 substantial amelioration of cold stress exposure throughout the snow-affected regions (Fig. 4b) but
 316 when snow effects were included there was little simulated change in cold stress exposure and, at

317 some sites, increased cold stress exposure occurred (Fig. 4b). For the endotherm simulation, mean
 318 hibernation costs were greatest in the Southern Rocky Mountain Steppe ecoregion (Fig. S4) and it
 319 was in this region that strongest reductions in hibernation costs occurred in contemporary times
 320 (Fig. 4d). Simulated warming of 1, 2 and 3 °C resulted an overall reduction in cold stress (cold stress
 321 exposure for lizards, total hibernation energy requirements for endotherms) as warming increased
 322 relative to the baseline 1980-2017 condition, but there were always some sites exhibiting an
 323 increase in cold stress with warming (Fig. 5).
 324

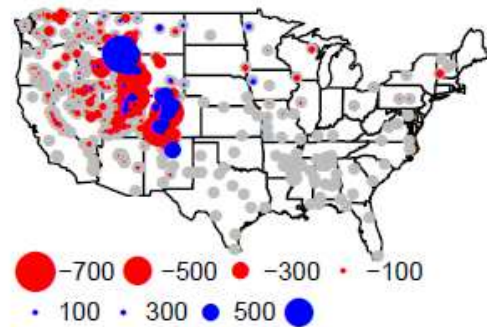


325
 326 **Figure 4.** Simulated historical (1980-2017) changes in a) activity level, b) exposure to cold stress (< -
 327 0.63 °C if snow simulated to be absent c) or present, for a thermoregulating lizard retreating to 5 cm
 328 depth, and d) overwinter hibernation costs for an endotherm retreating to the same depth. Grey
 329 points indicate sites with magnitude zero.
 330

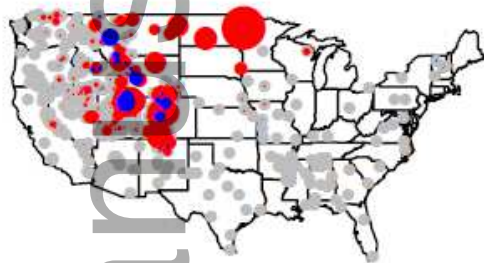
a) Δ freezing exposure ($^{\circ}$ days), +1 $^{\circ}$ C



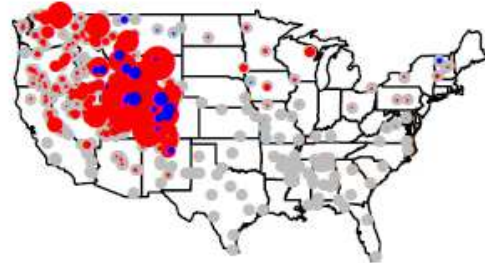
b) Δ hibernation cost (kJ), +1 $^{\circ}$ C



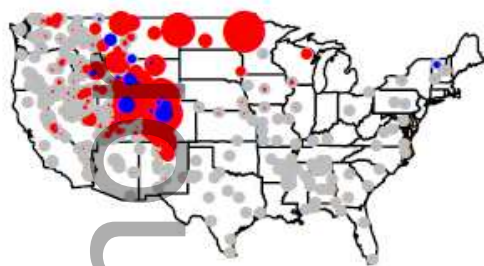
c) Δ freezing exposure ($^{\circ}$ days), +2 $^{\circ}$ C



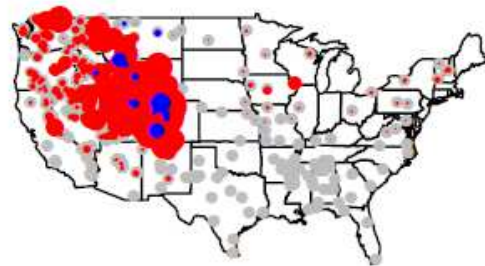
d) Δ hibernation cost (kJ), +2 $^{\circ}$ C



e) Δ freezing exposure ($^{\circ}$ days), +3 $^{\circ}$ C



f) Δ hibernation cost (kJ), +3 $^{\circ}$ C



331
332

333 **Figure 5.** Simulated air temperature warming effects (+1, +2 and +3 $^{\circ}$ C) on changes in lizard cold
334 stress (< -0.63 $^{\circ}$ C) exposure (a, c & e) and mammal hibernation costs (b, d & f) compared to base
335 1980-2017 environmental sequence for animals sheltering 5 cm underground. Red indicates a
336 decrease in exposure to cold stress/energy requirements compared to baseline, blue an increase.
337 Grey points indicate sites with magnitude zero.

338

339 **Discussion**

340

341 The NicheMapR microclimate modelling system provided robust representation of snow
342 accumulation and melting processes, and its feedbacks to soil temperature, across the USA. It was
343 able to predict snow depth and soil temperatures to within 15% of the observed range (Table 1, Fig.
344 1), without any site-specific details other than those available from gridded environmental data.
345 There is a wide range of snow models that vary in their representation of the environmental fluxes
346 and vertical processes within the snowpack (see, e.g., Avanzi *et al.*, 2016 and references therein).
347 The influence of snow on microclimates includes strong interactions and non-linearities, especially
348 relating to humidity, wind speed and solar radiation effects (e.g. Harpold & Brooks, 2018). Thus fully-
349 physical representations of the effect of snow on soil heat budgets should be more robust and
350 generalisable to novel environmental conditions. The NicheMapR scheme neglects some details of
351 the snow ripening process, such as water movement within the snowpack during freeze-thaw
352 events, depth-specific changes in density, as well as vertical changes in snow structure and
353 penetration of solar radiation. However, the present study shows that it can produce accurate
354 microclimatic predictions at the temporal and spatial scales relevant to organisms under the
355 influence of snow and can incorporate many terrain and landscape features that are important for
356 species-specific microclimates (e.g. shade, slope, aspect, hill shade, soil thermal and hydraulic
357 properties).
358
359 It was surprising that very little improvement was made on the predictions when site-specific details
360 were included in the parameterisation, with only soil moisture showing substantial improvements
361 (Table 1). However, there were some sites where soil temperature was clearly affected by shade,
362 and in these cases the site-specific predictions were more accurate (e.g. SCAN site 2146, 5 cm *rmsdp*
363 9.1% with shade and 11.4% without shade). The use of photographs to estimate microclimatic
364 conditions is of course not ideal and associated inaccuracies may have also contributed to the lack of
365 improvement from site-specific parameters; ideally one would make on-site measurements of these
366 parameters.
367
368 One of the main aims of this study was to generally quantify the effect of snow in decoupling soil
369 temperature from climate warming. There is a strong air temperature warming signal in the gridMET
370 dataset for the sites considered, especially those in the mountainous, inland snow-affected regions
371 (Fig. 2b), as is borne out in analyses of the raw station data (see Fig. S2b and Harpold & Brooks,
372 2018). All else being equal, this warming should lead to general decreases in snow cover and
373 duration (Isard *et al.*, 2007; Campbell *et al.*, 2010; Brown & DeGaetano, 2011), but such declines may
374 be offset by increased precipitation or reduced solar radiation via cloud effects. The actual snow

375 depth records are incomplete to various degrees, making it difficult to infer the degree of generality
376 of warming effects on snow dynamics. However, the gridMET data captures the relevant climatic
377 covariances and the simulation results predicted linear snow depth declines at almost one third of
378 sites (Fig. 2c) with a less extensive effect on snow duration (Fig. 2d).

379
380 Theory and observation predict that snow cover reductions should generally result in a greater risk
381 of exposure to freezing temperatures (e.g. Venn & Green, 2018). The simulated removal of snow
382 (Fig. 1 and Fig. S1) reduced soil temperature in a manner consistent with experimental snow removal
383 studies (Decker *et al.*, 2003; Wipf *et al.*, 2009; Chang *et al.*, 2014) and smaller-scale simulated
384 removals (Xu & Spitler, 2014). The buffering effect of snow on minimum temperature was generally
385 $> 10\text{ }^{\circ}\text{C}$, in some places as high as $19\text{ }^{\circ}\text{C}$ (Fig. S1). Accordingly, there was a strong decoupling between
386 air temperature warming, whether at 2 m (Fig. 2b) or 1 cm (Fig. 3a), and soil temperature warming
387 (Fig. 3b). The main effect was for the shallow soil temperature to warm at one third the rate of air
388 temperature, and for the exposure to cold stress conditions to be indifferent to the air temperature
389 warming. Few sites showed the paradoxical cooling effect of warming air temperature on shallow
390 soils (Fig. 3d & 4c), at least with respect to exposure to freezing. Zhang *et al.* (2005) undertook a
391 simulation study of a similar nature to the present study for Canada, using a monthly climatology as
392 forcing data. They inferred a similar damping effect of snow on the historical rate of warming of soil
393 when compared with air ($0.6\text{ }^{\circ}\text{C}$ and $1.0\text{ }^{\circ}\text{C}$, respectively, from 1900 to 1995) to that found in the
394 present study, and Zhang *et al.*'s simulated air temperature warming, and cooling experiments
395 showed a strong influence of feedbacks involving snow cover. In the present study, the decoupling
396 between soil and air temperature persisted even with a $3.0\text{ }^{\circ}\text{C}$ climate warming imposed on the
397 historical air temperature data (as reflected in simulated lizard exposure to cold stress, Fig. 5),
398 suggesting that this snow-mediated microclimatic effect will persist at least through the remainder
399 of this century.

400
401 The decoupling of air and soil temperatures will have many important ecological consequences. Here
402 I specifically investigated how it might influence ectothermic and endothermic animals, using a
403 biophysical model to compute activity time and exposure to cold stress in a lizard and hibernation
404 costs for a mammal over the study region and period. For the lizard, the contemporary warming
405 evident in the gridMET data had the effect of substantially increasing activity time at the sites
406 considered. This general beneficial effect of warming is contrary to previous work suggesting a
407 general reduction in activity time (Sinervo *et al.*, 2010). However, the calculations here assume that
408 shade is always available (Kearney *et al.*, 2009; see also Kearney, 2013; Walker *et al.*, 2015). Despite

409 the substantial increases in air temperature over this period, the exposure to temperatures below
410 the freezing state of tissue (~ -0.6 °C, Lowe *et al.*, 1971) were ameliorated at only 2 % of all sites.
411 Moreover, cold exposure increased at 2% of sites (Fig. 4c), specifically in regions where snow depth
412 and/or duration were predicted to have declined (Fig. 2c & d). In contrast, when the simulation was
413 run with the snow model switched off, so that precipitation never fell as snow but still fell as rain,
414 there was a strong linear decline in cold stress exposure under historical warming in snow-affected
415 regions (Fig. 4b & Fig. 2a).

416 For the mammal, there was a generally positive effect of contemporary warming in the form of
417 reduced hibernation costs (see Fig. 1). The absolute costs of hibernation, which must be met by
418 stored energy, depend on both the duration of the hibernation period and the temperatures
419 experienced during hibernation. Hibernation costs are minimised when a mammal is in the
420 thermoneutral zone of its lowest tolerable body temperature (Geiser, 2004) and, for the present
421 simulation (hibernation T_b of 2 °C for a 20 g mammal), the optimal ambient temperature for
422 hibernation was ~ 1.6 °C (see example in SI Text). The positive effects of climate warming on
423 hibernation costs in the present study were a result of both a reduced snow period (e.g. shortened
424 hibernation periods Fig. 1) but also especially through the snow buffering the hibernaculum
425 temperature to near 0 °C due to the latent heat of fusion.

426

427 Under climate warming up to 3 °C, cold stress is reduced for both ectotherms and endotherms at
428 many sites, but some sites experienced increases in cold stress (Fig. 5). These latter sites cluster in
429 the Southern Rocky Mountains Steppe ecoregion (Bailey, 1998), an area of high elevation and
430 relative low precipitation that has experienced some of the highest rates of contemporary warming
431 (Fig. 2b). This ecoregion therefore stands out as worthy of future attention in studies of the
432 ecological effects of climate warming.

433

434 The example simulations presented here are clearly not exhaustive but are illustrative of the fact
435 that the direct effects of snow-mediated microclimate on organismal physiology are idiosyncratic
436 and must take account of species-specific factors (e.g. overwinter sites, metabolic systems, cold
437 tolerance mechanisms). The ecological consequences of such physiological effects are difficult to
438 predict; for instance, they may benefit cold-tolerant species through an increased growth season
439 without losing a competitive edge against warm-adapted competitors or hinder them through
440 inappropriate phenological responses. Thus, snow-mediated changes to the coupling of soil and air
441 temperature under climate warming, as presented here and reported an increasing number of
442 empirical and simulation studies around the world (Decker *et al.*, 2003; Zhang *et al.*, 2005; Wipf *et*

443 *al.*, 2009; Chang *et al.*, 2014; Xu & Spitler, 2014; Aalto *et al.*, 2018), will pose unique adaptive
444 challenges. This will be especially the case for organisms spanning the soil/air interface physically
445 (plants), behaviourally (e.g. underground retreats) or through ontogeny (e.g. eggs vs. adults).
446 Ecologists studying snow-affected systems therefore need accessible tools to capture the underlying
447 micrometeorological processes. The modelling framework developed here should provide an
448 accessible means for ecologists to make accurate inferences of the microclimatic consequences of
449 snow on biological processes in the USA and beyond (Kearney *et al.*, 2019).

450

451 **References**

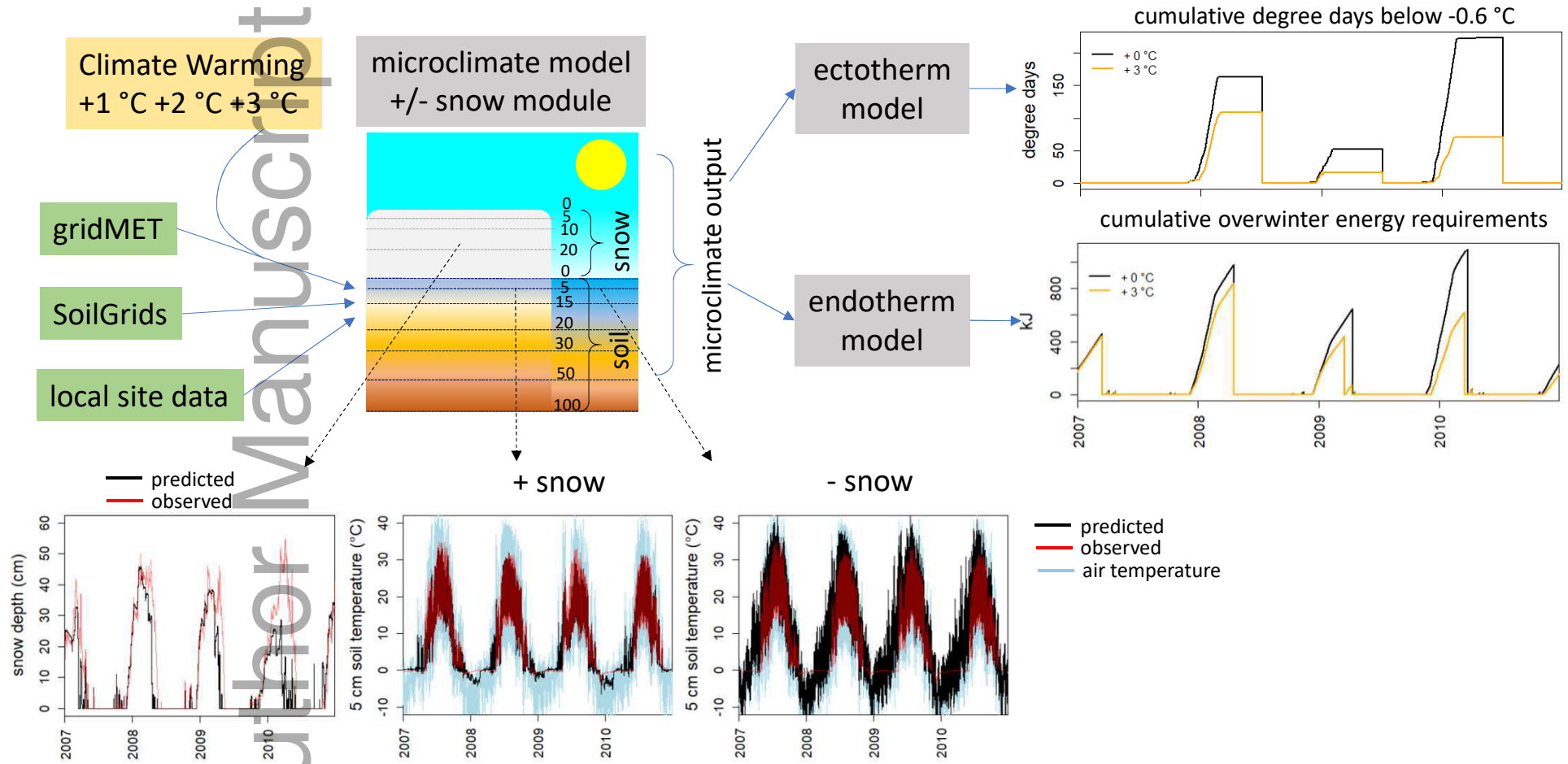
- 452 Aalto, J., Scherrer, D., Lenoir, J., Guisan, A. & Luoto, M. (2018) Biogeophysical controls on soil-
453 atmosphere thermal differences: implications on warming Arctic ecosystems. *Environmental*
454 *Research Letters*, **13**, 074003.
- 455 Abatzoglou, J.T. (2013) Development of gridded surface meteorological data for ecological
456 applications and modelling. *International Journal of Climatology*, **33**, 121–131.
- 457 Anderson, E. (2006) Snow Accumulation and Ablation Model - SNOW-17.
- 458 Avanzi, F., De Michele, C., Ghezzi, A., Jommi, C. & Pepe, M. (2014) A processing–modeling routine to
459 use SNOTEL hourly data in snowpack dynamic models. *Advances in Water Resources*, **73**, 16–
460 29.
- 461 Avanzi, F., Michele, C.D., Morin, S., Carmagnola, C.M., Ghezzi, A. & Lejeune, Y. (2016) Model
462 complexity and data requirements in snow hydrology: seeking a balance in practical
463 applications. *Hydrological Processes*, **30**, 2106–2118.
- 464 Bailey, R.G. (1998) *Ecoregions; The ecosystem geography of the oceans and continents*, Springer-
465 Verlag, New York.
- 466 Bale, J.S. & Hayward, S.A.L. (2010) Insect overwintering in a changing climate. *Journal of*
467 *Experimental Biology*, **213**, 980–994.
- 468 Bartlett, P.A., MacKay, M.D. & Verseghy, D.L. (2006) Modified snow algorithms in the Canadian land
469 surface scheme: Model runs and sensitivity analysis at three boreal forest stands.
470 *Atmosphere-Ocean*, **44**, 207–222.
- 471 Brown, P.J. & DeGaetano, A.T. (2011) A paradox of cooling winter soil surface temperatures in a
472 warming northeastern United States. *Agricultural and Forest Meteorology*, **151**, 947–956.
- 473 Campbell, G.S. & Norman, J.M. (1998) *Environmental Biophysics*, Springer, New York.
- 474 Campbell, J.L., Ollinger, S.V., Flerchinger, G.N., Wicklein, H., Hayhoe, K. & Bailey, A.S. (2010) Past and
475 projected future changes in snowpack and soil frost at the Hubbard Brook Experimental
476 Forest, New Hampshire, USA. *Hydrological Processes*, **24**, 2465–2480.

- 477 Chang, J., Wang, G., Gao, Y. & Wang, Y. (2014) The influence of seasonal snow on soil thermal and
478 water dynamics under different vegetation covers in a permafrost region. *Journal of*
479 *Mountain Science*, **11**, 727–745.
- 480 Cosby, B.J., Hornberger, G.M., Clapp, R.B. & Ginn, T.R. (1984) A Statistical Exploration of the
481 Relationships of Soil Moisture Characteristics to the Physical Properties of Soils. *Water*
482 *Resources Research*, **20**, 682–690.
- 483 Cuntz, M. & Haverd, V. (2018) Physically Accurate Soil Freeze-Thaw Processes in a Global Land
484 Surface Scheme. *Journal of Advances in Modeling Earth Systems*, **10**, 54–77.
- 485 Decker, K.L.M., Wang, D., Waite, C. & Scherbatskoy, T. (2003) Snow Removal and Ambient Air
486 Temperature Effects on Forest Soil Temperatures in Northern Vermont. *Soil Science Society*
487 *of America Journal*, **67**, 1234.
- 488 Essery, R., Morin, S., Lejeune, Y. & B Ménard, C. (2013) A comparison of 1701 snow models using
489 observations from an alpine site. *Advances in Water Resources*, **55**, 131–148.
- 490 Geiser, F. (2004) Metabolic Rate and Body Temperature Reduction During Hibernation and Daily
491 Torpor. *Annual Review of Physiology*, **66**, 239–274.
- 492 Groffman, P.M., Driscoll, C.T., Fahey, T.J., Hardy, J.P., Fitzhugh, R.D. & Tierney, G.L. (2001) Colder
493 soils in a warmer world: A snow manipulation study in a northern hardwood forest
494 ecosystem. *Biogeochemistry*, **56**, 135–150.
- 495 Hamman, J.J., Nijssen, B., Bohn, T.J., Gergel, D.R. & Mao, Y. (2018) The Variable Infiltration Capacity
496 model version 5 (VIC-5): infrastructure improvements for new applications and
497 reproducibility. *Geoscientific Model Development*, **11**, 3481–3496.
- 498 Harpold, A.A. & Brooks, P.D. (2018) Humidity determines snowpack ablation under a warming
499 climate. *Proceedings of the National Academy of Sciences*, **115**, 1215–1220.
- 500 Hengl, T., de Jesus, J.M., Heuvelink, G.B., Gonzalez, M.R., Kilibarda, M., Blagotić, A., Shanguan, W.,
501 Wright, M.N., Geng, X., Bauer-Marschallinger, B. & others (2017) SoilGrids250m: Global
502 gridded soil information based on machine learning. *PLoS one*, **12**, e0169748.
- 503 Hengl, T., de Jesus, J.M., MacMillan, R.A., Batjes, N.H., Heuvelink, G.B.M., Ribeiro, E., Samuel-Rosa,
504 A., Kempen, B., Leenaars, J.G.B., Walsh, M.G. & Gonzalez, M.R. (2014) SoilGrids1km —
505 Global Soil Information Based on Automated Mapping. *PLoS ONE*, **9**, e105992.
- 506 Isard, S.A., Schaetzl, R.J. & Andresen, J.A. (2007) Soils Cool as Climate Warms in the Great Lakes
507 Region: 1951–2000. *Annals of the Association of American Geographers*, **97**, 467–476.
- 508 ávila-Jiménez, M.L., Coulson, S.J., Solhøy, T. & Sjöblom, A. (2010) Overwintering of terrestrial Arctic
509 arthropods: the fauna of Svalbard now and in the future. *Polar Research*, **29**, 127–137.

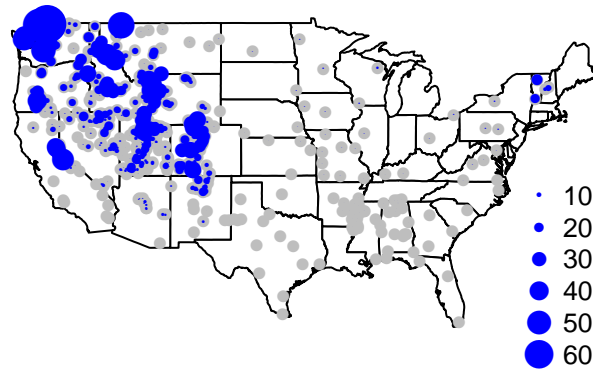
- 510 Jones, D., Wang, W. & Fawcett, R. (2009) High-quality spatial climate data-sets for Australia.
511 *Australian Meteorological and Oceanographic Journal*, **58**, 233–248.
- 512 Jordan, R. (1991) *A one-dimensional temperature model for a snow cover: Technical documentation*
513 *for SNTHERM.89*, U.S. Army Corps of Engineers: Cold Regions Research & Engineering
514 Laboratory.
- 515 Kearney, M., Shine, R. & Porter, W.P. (2009) The potential for behavioral thermoregulation to buffer
516 “cold-blooded” animals against climate warming. *Proceedings of the National Academy of*
517 *Sciences*, **106**, 3835–3840.
- 518 Kearney, M.R. (2013) Activity restriction and the mechanistic basis for extinctions under climate
519 warming. *Ecology Letters*, **16**, 1470–1479.
- 520 Kearney, M.R., Gillingham, P.K., Bramer, I., Duffy, J.P. & Maclean, I.M.D. (2019) A method for
521 computing hourly, historical, terrain-corrected microclimate anywhere on Earth. *Methods in*
522 *Ecology and Evolution*.
- 523 Kearney, M.R. & Maino, J.L. (2018) Can next-generation soil data products improve soil moisture
524 modelling at the continental scale? An assessment using a new microclimate package for the
525 R programming environment. *Journal of Hydrology*, **561**, 662–673.
- 526 Kearney, M.R. & Porter, W.P. (2019) NicheMapR - an R package for biophysical modelling: the
527 ectotherm and Dynamic Energy Budget models. *Ecography*, **42**, 1–12.
- 528 Kearney, M.R. & Porter, W.P. (2017) NicheMapR - an R package for biophysical modelling: the
529 microclimate model. *Ecography*, **40**, 664–674.
- 530 Kearney, M.R., Shamakhly, A., Tingley, R., Karoly, D.J., Hoffmann, A.A., Briggs, P.R. & Porter, W.P.
531 (2014) Microclimate modelling at macro scales: a test of a general microclimate model
532 integrated with gridded continental-scale soil and weather data. *Methods in Ecology and*
533 *Evolution*, **5**, 273–286.
- 534 Kemp, M.U., Emiel van Loon, E., Shamoun-Baranes, J. & Bouten, W. (2012) RNCEP: global weather
535 and climate data at your fingertips: RNCEP. *Methods in Ecology and Evolution*, **3**, 65–70.
- 536 Körtner, G. & Geiser, F. (1998) Ecology of natural hibernation in the marsupial mountain pygmy-
537 possum (*Burramys parvus*). *Oecologia*, **113**, 170–178.
- 538 Liston, G.E. & Sturm, M. (1998) A snow-transport model for complex terrain. *Journal of Glaciology*,
539 **44**, 498–516.
- 540 Lowe, C.H., Lardner, P.J. & Halpern, E.A. (1971) Supercooling in reptiles and other vertebrates.
541 *Comparative Biochemistry and Physiology Part A: Physiology*, **39**, 125–135.

- 542 Lute, A.C. & Luce, C.H. (2017) Are Model Transferability And Complexity Antithetical? Insights From
543 Validation of a Variable-Complexity Empirical Snow Model in Space and Time. *Water*
544 *Resources Research*, **53**, 8825–8850.
- 545 Monson, R.K., Lipson, D.L., Burns, S.P., Turnipseed, A.A., Delany, A.C., Williams, M.W. & Schmidt, S.K.
546 (2006) Winter forest soil respiration controlled by climate and microbial community
547 composition. *Nature*, **439**, 711.
- 548 New, M., Lister, D., Hulme, M. & Makin, I. (2002) A high-resolution data set of surface climate over
549 global land areas. *Climate Research*, **21**, 1–25.
- 550 Pauli, J.N., Zuckerberg, B., Whiteman, J.P. & Porter, W. (2013) The subnivium: a deteriorating
551 seasonal refugium. *Frontiers in Ecology and the Environment*, **11**, 260–267.
- 552 Porter, W.P. & Kearney, M. (2009) Size, shape, and the thermal niche of endotherms. *Proceedings of*
553 *the National Academy of Sciences*, **106**, 19666–19672.
- 554 Ruddell, A.R., Budd, W.F., Smith, I.N., Keage, P.L. & Jones, R. (1990) *The south east Australian alpine*
555 *climate study*, The University of Melbourne and the Department of Meteorology an Alpine
556 Resorts Commission, Victoria, Melbourne, Victoria.
- 557 Sanders-DeMott, R., Campbell, J.L., Groffman, P.M., Rustad, L.E. & Templer, P.H. (2019) *Soil warming*
558 *and winter snowpacks: Implications for northern forest ecosystem functioning. Ecosystem*
559 *Consequences of Soil Warming*, pp. 245–278. Elsevier.
- 560 Sanders-DeMott, R., McNellis, R., Jabouri, M. & Templer, P.H. (2018) Snow depth, soil temperature
561 and plant-herbivore interactions mediate plant response to climate change. *Journal of*
562 *Ecology*, **106**, 1508–1519.
- 563 Schaefer, G.L., Cosh, M.H. & Jackson, T.J. (2007) The USDA Natural Resources Conservation Service
564 Soil Climate Analysis Network (SCAN). *Journal of Atmospheric and Oceanic Technology*, **24**,
565 2073–2077.
- 566 Serreze, M.C., Clark, M.P., Armstrong, R.L., McGinnis, D.A. & Pulwarty, R.S. (1999) Characteristics of
567 the western United States snowpack from snowpack telemetry (SNOTEL) data. *Water*
568 *Resources Research*, **35**, 2145–2160.
- 569 Sinervo, B., Mendez-de-la-Cruz, F., Miles, D.B., Heulin, B., Bastiaans, E., Villagran-Santa Cruz, M.,
570 Lara-Resendiz, R., Martinez-Mendez, N., Calderon-Espinosa, M.L., Meza-Lazaro, R.N.,
571 Gadsden, H., Avila, L.J., Morando, M., De la Riva, I.J., Sepulveda, P.V., Rocha, C.F.D.,
572 Ibarquengoytia, N., Puntriano, C.A., Massot, M., Lepetz, V., Oksanen, T.A., Chapple, D.G.,
573 Bauer, A.M., Branch, W.R., Clobert, J. & Sites, J.W., Jr. (2010) Erosion of Lizard Diversity by
574 Climate Change and Altered Thermal Niches. *Science*, **328**, 894–899.

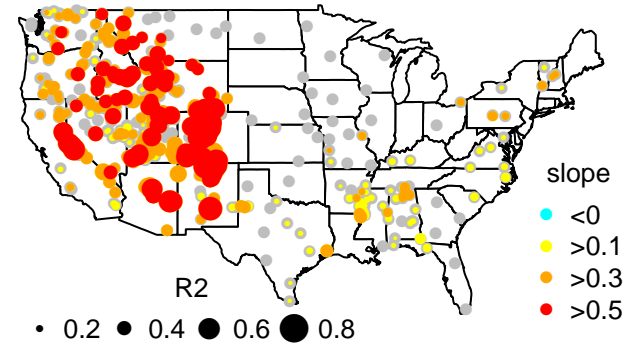
- 575 Sinha, T. & Cherkauer, K.A. (2010) Impacts of future climate change on soil frost in the midwestern
576 United States. *Journal of Geophysical Research: Atmospheres*, **115**.
- 577 Sturm, M., Taras, B., Liston, G.E., Derksen, C., Jonas, T. & Lea, J. (2010) Estimating Snow Water
578 Equivalent Using Snow Depth Data and Climate Classes. *Journal of Hydrometeorology*, **11**,
579 1380–1394.
- 580 Thompson, K.L., Zuckerberg, B., Porter, W.P. & Pauli, J.N. (2018) The phenology of the subnivium.
581 *Environmental Research Letters*.
- 582 Venn, S.E. & Green, K. (2018) Evergreen alpine shrubs have high freezing resistance in spring,
583 irrespective of snowmelt timing and exposure to frost: an investigation from the Snowy
584 Mountains, Australia. *Plant Ecology*, **219**, 209–216.
- 585 Walker, S., Stuart-Fox, D. & Kearney, M.R. (2015) Has contemporary climate change played a role in
586 population declines of the lizard *Ctenophorus decresii* from semi-arid Australia? *Journal of*
587 *Thermal Biology*, **54**, 66–77.
- 588 Warming, Eugenius (1909) *Oecology of plants : an introduction to the study of plant-communities*,
589 Oxford :Clarendon Press,.
- 590 Wipf, S., Stoeckli, V. & Bebi, P. (2009) Winter climate change in alpine tundra: plant responses to
591 changes in snow depth and snowmelt timing. *Climatic Change*, **94**, 105–121.
- 592 Xu, H. & Spitler, J.D. (2014) The relative importance of moisture transfer, soil freezing and snow
593 cover on ground temperature predictions. *Renewable Energy*, **72**, 1–11.
- 594 Zhang, T. (2005) Influence of the seasonal snow cover on the ground thermal regime: An overview.
595 *Reviews of Geophysics*, **43**, n/a-n/a.
- 596 Zhang, Y. (2003) A process-based model for quantifying the impact of climate change on permafrost
597 thermal regimes. *Journal of Geophysical Research*, **108**, 4695.
- 598 Zhang, Y., Chen, W., Smith, S.L., Riseborough, D.W. & Cihlar, J. (2005) Soil temperature in Canada
599 during the twentieth century: Complex responses to atmospheric climate change. *Journal of*
600 *Geophysical Research: Atmospheres*, **110**, 1-15.
- 601



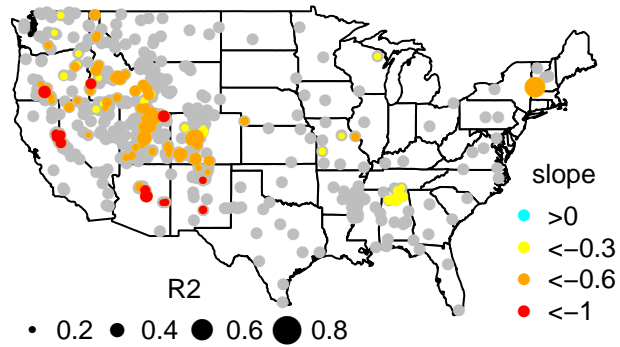
a) mean annual snow depth (cm)



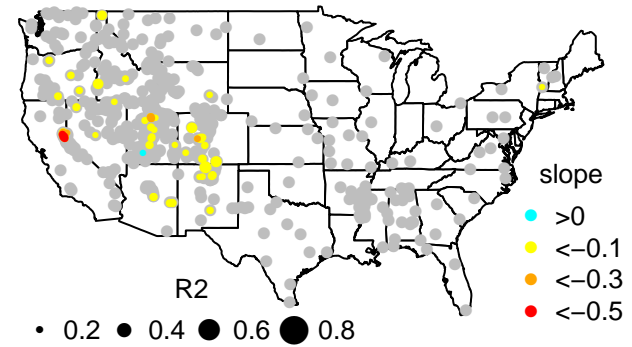
b) warming rate ($^{\circ}\text{C}/\text{decade}$), 2m air



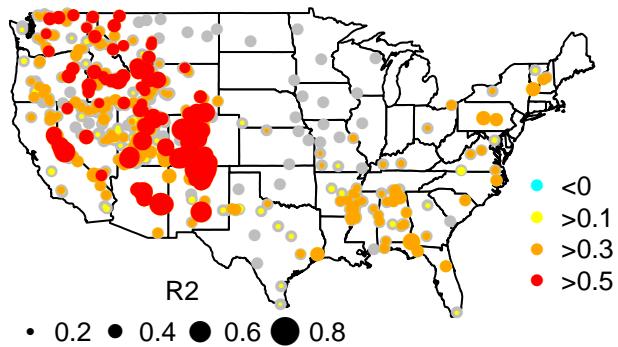
c) delta mean snow depth (cm/y)



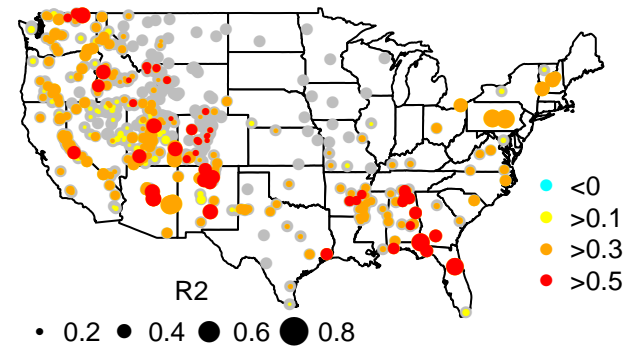
d) delta mean snow days (d/y)



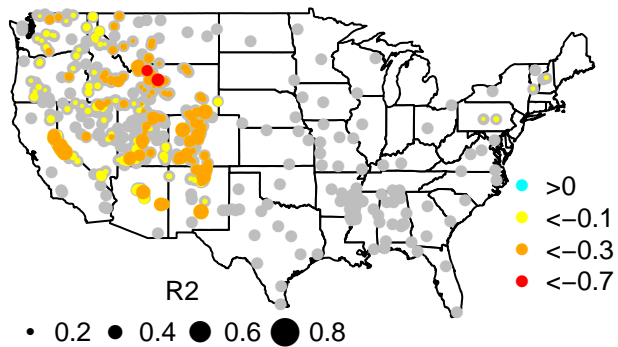
a) warming rate ($^{\circ}\text{C}/\text{decade}$), 1cm air



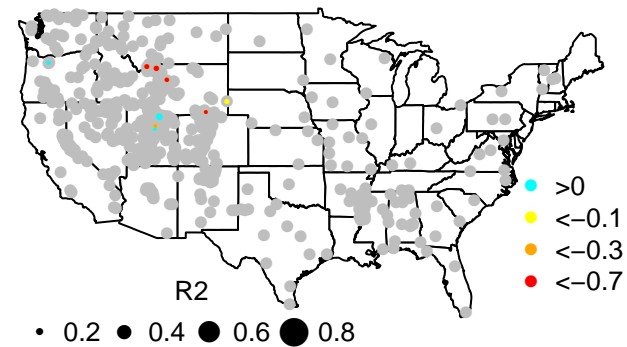
b) warming rate ($^{\circ}\text{C}/\text{decade}$), 5cm soil

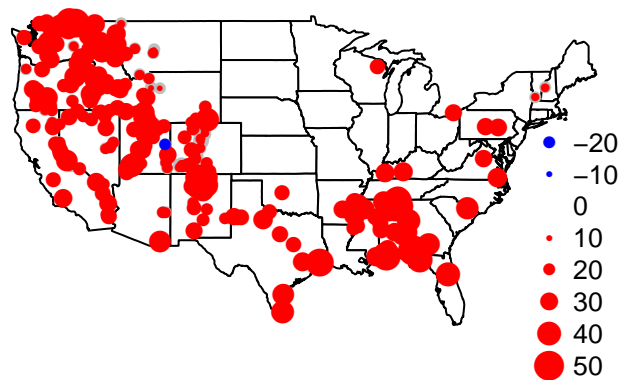
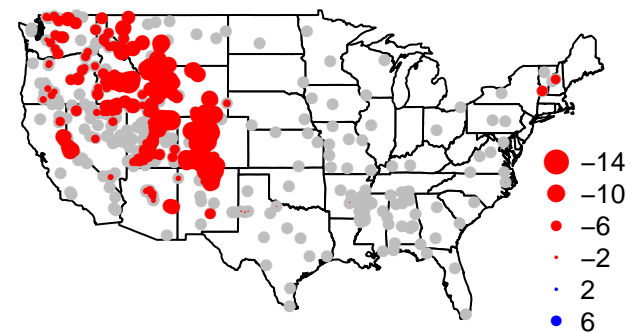
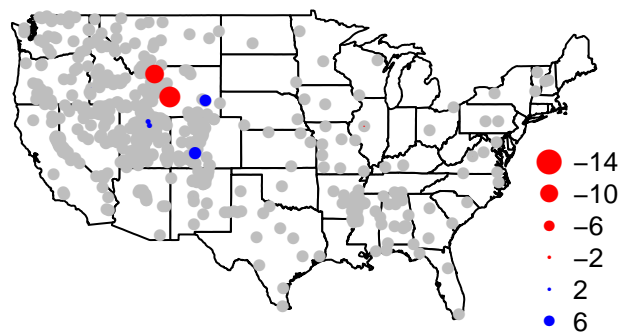
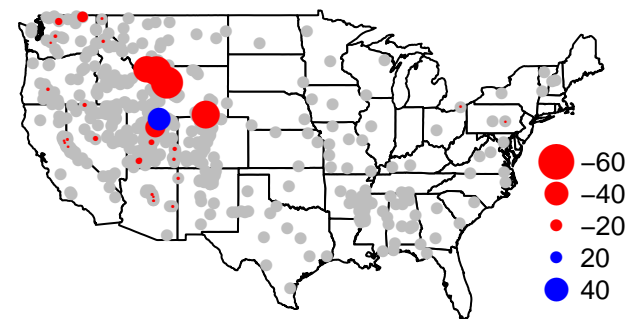


c) delta $^{\circ}\text{days}$ freezing 1cm air (d/y)



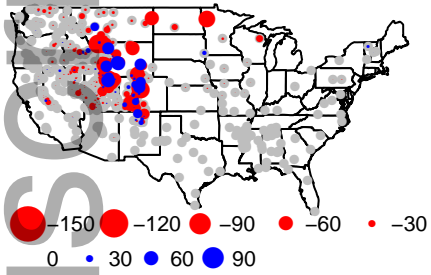
d) delta $^{\circ}\text{days}$ freezing 5cm soil (d/y)



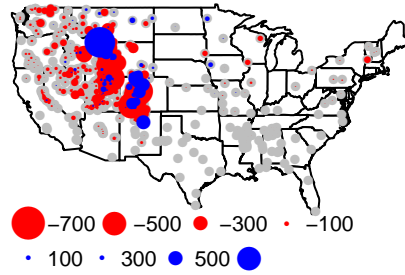
a) Δ lizard activity time (hours/decade)b) Δ freezing exposure ($^{\circ}$ days/year) without snowc) Δ freezing exposure ($^{\circ}$ days/year) with snowd) Δ mammal hibernation cost (kJ/year)

Preprint
 Manuscript
 Author

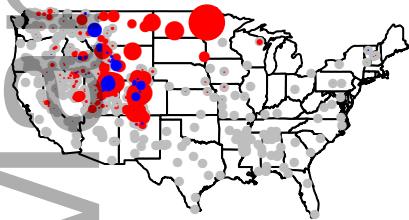
a) Δ freezing exposure ($^{\circ}$ days), +1 $^{\circ}$ C



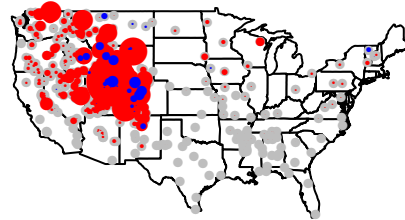
b) Δ hibernation cost (kJ), +1 $^{\circ}$ C



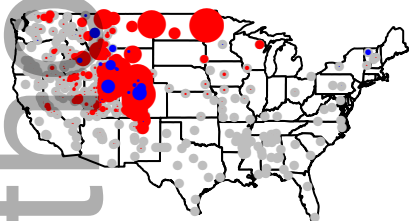
c) Δ freezing exposure ($^{\circ}$ days), +2 $^{\circ}$ C



c) Δ hibernation cost (kJ), +2 $^{\circ}$ C



e) Δ freezing exposure ($^{\circ}$ days), +3 $^{\circ}$ C



f) Δ hibernation cost (kJ), +3 $^{\circ}$ C

